MACHINING OF CFRP: DRILLING AND MILLING OF UNSTABLE WORK PIECES

Fabian Lissek [1], Michael Kaufeld [1], Jean-Pierre Bergmann [2]

[1]Institute of Production Engineering and Materials Testing, Ulm University of Applied Sciences, Prittwitzstraße 10, 89075 Ulm, Germany
[2]Department of Production Technology, Ilmenau University of Technology, Neuhaus 1, 98693 Ilmenau, Germany

ABSTRACT

The machining of near net shape carbon fiber reinforced polymers (CFRP) still causes high costs with regard to tool wear and clamping methods. Especially clamping systems used in industry offer potential to reduce costs by gripping the work pieces partial and not fully supported. Therefore this paper deals with the machining of unstable CFRP-structures. The characteristic processes at drilling and trimming compliant work pieces are analyzed and the interactions between the cutting tool and the unsupported work piece are presented. In particular the delamination mechanism is decisive for the parameters which enable these production methods. As an unstable behavior of the work piece promotes the formation of damages, it is necessary to develop a limiting criterion for choosing suitable machining conditions. One approach for the drilling process is the use of an energy balance, taking into account the elastic energy stored in an unstable work piece. In the following article this possibility is investigated and evaluated experimentally by means of tool wear studies with unsupported work pieces.

Index Terms – CFRP, drilling, milling, unstable, delamination, step drill, multi-tooth cutter

1. INTRODUCTION

1.1 Motivation

Over the past decades the usage of lightweight materials, especially carbon fiber reinforced polymers (CFRP), has become more and more important in aerospace, automotive and energy production industries. In particular, because of their excellent weight to strength ratio, composite materials outperform metals and unreinforced plastics in many fields of application. Despite competing technologies, like water jet or laser cutting, the machining of near net shape composite material work pieces is still an important step in the process chain. Concerning this matter, the drilling operation, as a preparation for screw or rivet joints, and the contour milling are two of the most significant machining procedures. The quality requirements on work piece cutting edges are demanding, but meanwhile they can be met. Especially degradations like delamination, fiber projections and fraying are generally not accepted and have to be avoided. Therefore, the implementation of the cutting process requires very complex and cost-intensive clamping techniques. Classic holding devices like mechanical and hydraulic systems are used as well as modular vacuum clamping systems. The complexity of these appliances results from the demand to avoid effects like work piece vibrations by introducing the clamping forces as near as possible at the machining point [Enß13].

A possible solution to reduce costs and complexity of present clamping systems would be, to machine composite materials unsupported in specified limits, or rather to tolerate a specific compliance of the work piece at the operating point [Lis13]. For the realization of this kind of a machining process, the interactions between the cutting tool and the unstable work piece have to be analyzed, as well as it is needed to determine the conditions necessary to achieve acceptable cutting results.

1.2 State of the art

Delamination is one of the most critical damages at machining composite materials [Abr07]. Generally every broken fiber weakens the compound structure. This effect is amplified by delaminated layers and in consequence the mechanical strength of the work piece is reduced [Per97]. The plies of the material can delaminate whenever a composite structure is stressed outwards in its thickness direction during the cutting process. The particular reason for this effect depends on several mechanisms of the different machining processes. For the drilling process, the peel-up delamination at the entry side and the push-down delamination at the exit side of the work piece are distinguished (Fig. 1) [Hoc90]. Peel-up delamination results from negative feed forces generated by the tools spiral grooves. While the top layer of the laminate is stripped off, the remaining layers are pressed to the opposite side by the feed force. However the push-down delamination at the exit side shows a considerably more distinctive extent of damage. When the remaining bottom layers are not supported anymore, the feed force exceeds the interlaminar strength and interlaminar fractures occur [Col91]. Thereby, the chisel edge has no cutting effect and induces the main part of the feed force [Won02]. Especially the abrasive wear of the cutting edges has a significant influence on the damage. A rounding of the main cutting edge increases the cutting force and thus also its component in the laminates thickness direction [Kha10]. The feed forces of the trimming operation by contour milling point into the direction of the laminate planes, so the delamination mechanism can be compared with the peel-up delamination from the drilling process, which is primarily caused by the tools spiral angle.

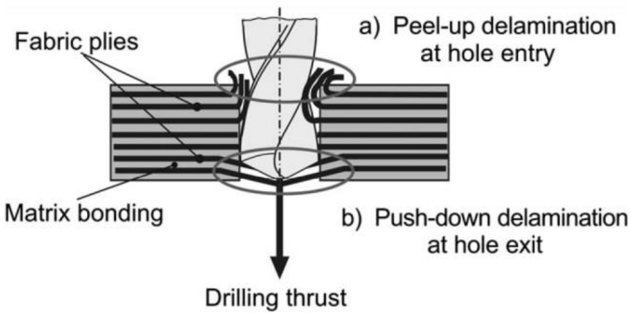

Fig. 1 – Delamination mechanisms at drilling CFRP [Far09]

High feed forces are assumed to be the main cause for delamination. It has been shown that a critical feed force should not be exceeded for delamination-free drilling of CFRP-work pieces [Hoc05]. Therefore, Hocheng and Dharan developed an analytic model to calculate the critical feed force, taking into account the linear-elastic fracture mechanics and plates theory [Hoc90]. Subsequently this model was extended in various publications to estimate the critical feed force for several tool geometries [Hoc03] and processing steps like pre-drilling [Tsa03]. A comparable approach for the milling process is not yet established, but Hartmann used the energy balance of the mentioned model to transfer it to the milling process [Har12]. However the author concluded that a continuous process monitoring system to control the cutting forces responsible for the crack extension is not possible.

First investigations regarding the machining of unstable CFRP-structures where performed by Capello [Cap04], who showed that the theory of the critical feed force is not valid for compliant work pieces. When the chisel edge exits the work piece the relative feed force increases and at the same time the load is redirected to the main cutting edges. This action supports the delamination effect and makes the damage process more complex. The machining process is temporarily transferred into a stamping process. In his work Capello presents a damping system, which prevents the change of the relative feed speed and avoids work piece degradations this way.

2. EXPERIMENTAL SETUP

2.1 Tools, materials and parameters

Table 1 summarizes the relevant parameters for the machining experiments. The step drills used, had a point angle σ from 70° up to 130° and a helix angle λ of 35°. The pre-drilling diameter d was 3.9 mm, widened up to a diameter D of 5.9 mm in the secondary drilling stage. For the milling experiments two different kinds of milling tools were used: Three double-edged cutters with helix angles varying from -5° to +5° and a multi-tooth milling tool with 30° right- and left-hand spiral. To analyze the influence of abrasive tool wear on unsupported machining, all tools were made of tungsten carbide without coating.

Table 1 – Tools, materials and parameters

	Drilling experiments	Milling experiments	
Tool type	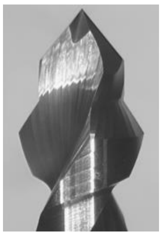 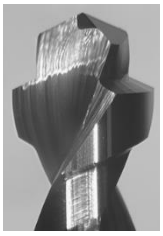 Step drill	 Multi-tooth	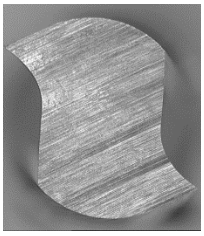 Two-edged
Point angle σ [°]	70 - 130	-	-
Spiral angle λ [°]	35	30/30	-5 ; +5 ; 0
Tool name	B70, …, B130	F1	$F2_{-5\,;\,0\,;\,+5}$
Cutting material	Tungsten carbide	Tungsten carbide	Tungsten carbide
Diameter d ; D [mm]	3.9 ; 5.9	- ; 8	- ; 8
Cutting speed v_c [m/min]	100	88	88
Feed rate f [mm/rev]	0.06	0.04	0.07
Work piece material	HexPly® UD/M21/35%/196/T800S 24 layers ; t = 4.3 mm $[-45, 90, 45, 0]_6$	HexPly® UD/M21/35%/268/T800S 8 layers ; t = 2.0 mm $[-45, 90, 45, 0]_2$	

The CFRP specimens had a quasi-isotropic structure and a symmetrical stacking sequence with a total height of 4.3 mm or 2.0 mm. The laminate was cured by means of an autoclave process using an epoxy prepreg with an intermediate modulus carbon fiber. The individual plies had a weight per unit area of 268 g/m^2 and 196 g/m^2 respectively, leading to a resin content of 35 % by weight. The experimental setup is shown in Fig. 2. The unstable work pieces were modeled as a one side fastened bending beam with a maximum possible dimension of 300 mm × 100 mm. The flexibility of the work piece was influenced by varying the material strength t or the unsupported length x.

The specimens were fixed on a clamping system mounted on a load cell, which measures the forces in three spatial directions (F_x, F_y, F_z). The cutting torque M_z was measured by a cutting force dynamometer, while a laser sensor measured the deflection f of the work piece during the whole machining process.

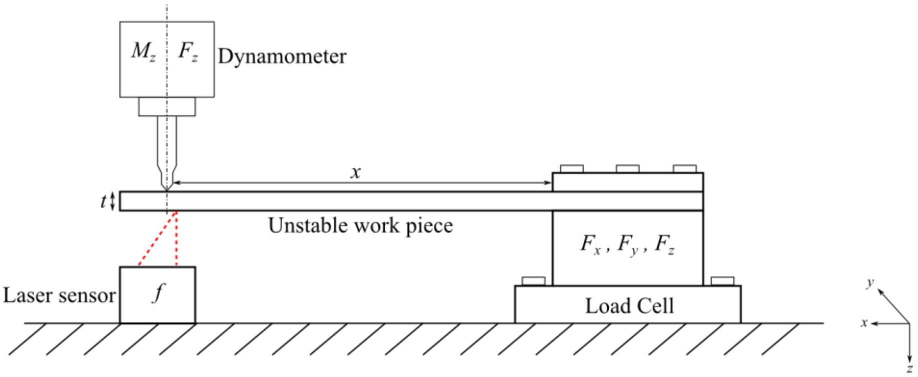

Fig. 2 – Experimental setup for the machining of unstable CFRP- work pieces

2.2 Supported and unsupported drilling with a step drill

For a better understanding of subsequent investigations the differences between supported and unsupported drilling with a step drill should be discussed here. To compare the two different drilling mechanisms, Fig. 3 shows the thrust force F_z as a function of the drilling time in two different situations. For a drilling position of x = 10 mm it can be assumed that the work piece is completely stable whereas an unsupported length of 160 mm demonstrates an example for an unsupported drilling process.

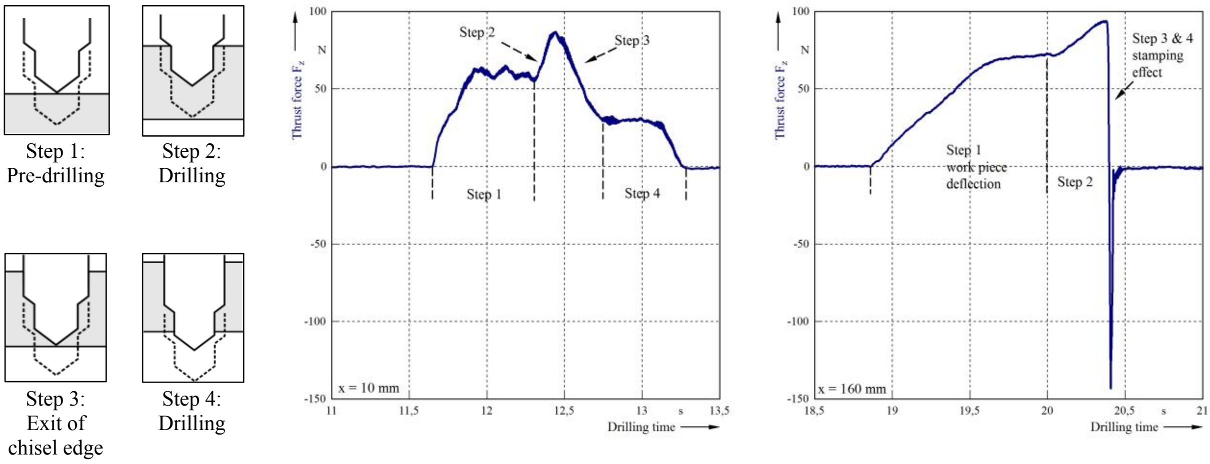

Fig. 3 – Thrust force *for supported (x = 10 mm) and unsupported (x = 160 mm) drilling with a step drill (f = 0,06 mm/rev ; v_c = 100 m/min ; σ = 115° ; t = 4.3 mm)*

The supported drilling process with a step drill may be divided into multiple sections. First of all the thrust force increases instantly while the chisel edge is penetrating the top layer of the material. As soon as the main cutting edges are engaged, the pre-drilling process starts. In this primary stage the thrust force reaches a constant level until the secondary drilling stage begins. Thereupon the thrust force is increasing a second time until the chisel edge breaks through the bottom layer, whereby the thrust force decreases strongly. Once the main cutting edges have left the material completely, the thrust force reaches a constant level in the secondary drilling stage as well. Due to the flexibility of an unstable work piece, the bending beam is moving in the same direction as the drill point.

Hence, the graph shows a slowly increasing thrust force during Step 1. Because of the strong reduction of the feed force as the chisel edge exits the bottom layer, the elastic force leads to a drastic raise of the relative feed speed. Before the work piece reaches zero position again, the machining process is comparable to a stamping process. Although delamination occurs at lower feed forces during unsupported drilling, it is possible to reach a good quality while machining beneath a certain threshold area. Fig. 4 shows the maximum cutting torque M_z of three drilling tools with differing point angles and compares the damage extent at two different drilling positions.

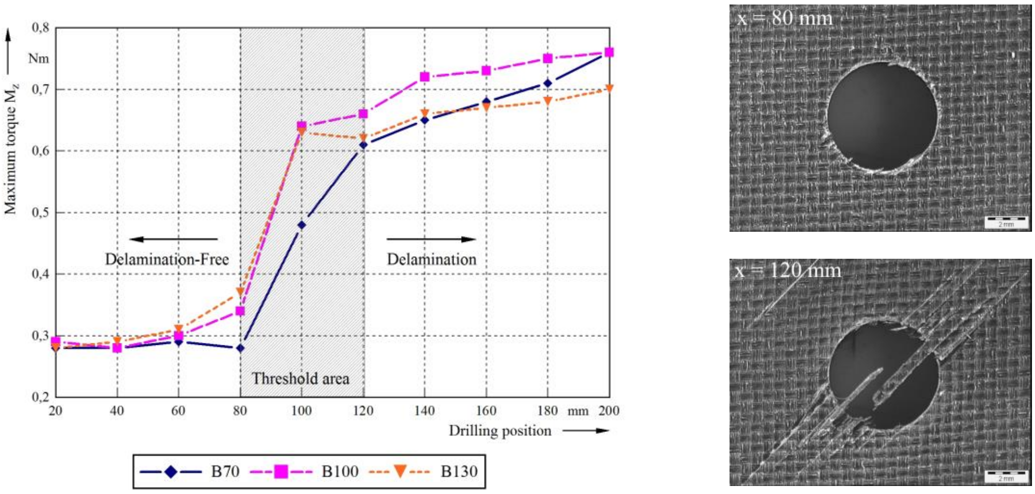

Fig. 4 – Maximum torque in the threshold area
(f = 0.06 mm/rev ; v_c = 100 m/min ; σ = 70°, 100°,130° ; t = 4.3 mm ; Magnification = 8.4x)

The graph demonstrates clearly that the rising of the cutting torque from 0.3 Nm to 0.7 Nm is independent from the tool geometry. At drilling positions with $x > 80$ mm an increasing maximum cutting torque occurs, while the maximum feed force at these drilling positions is approximately equal. In exactly the same way as the cutting torque rises, there is a higher local work piece compliance of the bending beam. Regarding to the cutting torque, this means that the compliance reached a level, which leads to a subsequent machining of the bore hole inner wall due to the circumference cutting edges. Particularly, this procedure, comparatively described as a reaming process, has certain effects on the shape accuracy of the bore holes. Fig. 5 shows the resulting deviations measured by confocal microscopy.

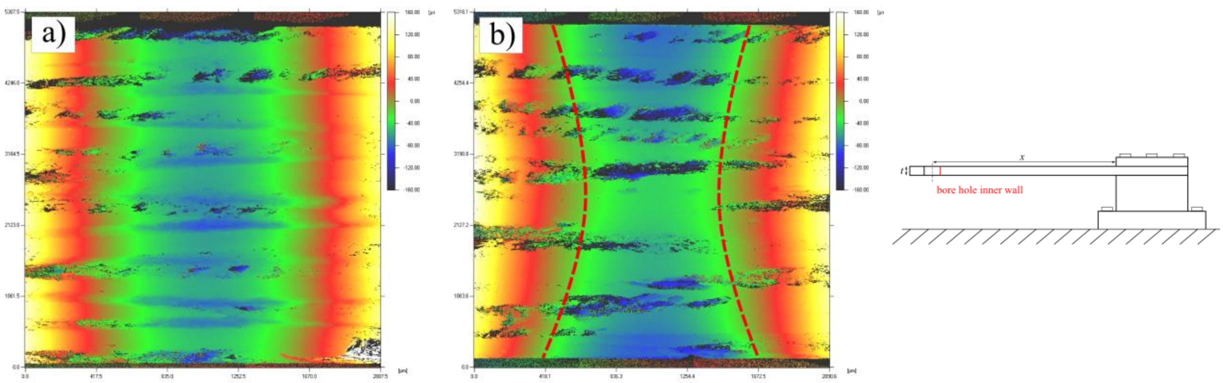

Fig. 5 – Deviation of the shape accuracy
a) x = 40 mm ; σ = 130°, b) x = 160 mm ; σ = 130°

The affected bore hole inner wall topographically looks like a constricted cylinder. Because of the minor work piece compliance, this effect is not recognizable after drilling with lower unsupported lengths. In general, all experiments have been performed under the condition to achieve bore hole dimensions within the general tolerance after DIN ISO 2768 [DIN2768]. Considering unsupported drilling processes with different point angles, the feed force and thus the feed rate is affected significantly by the tool geometry and the tool wear. Fig. 6 shows these relations.

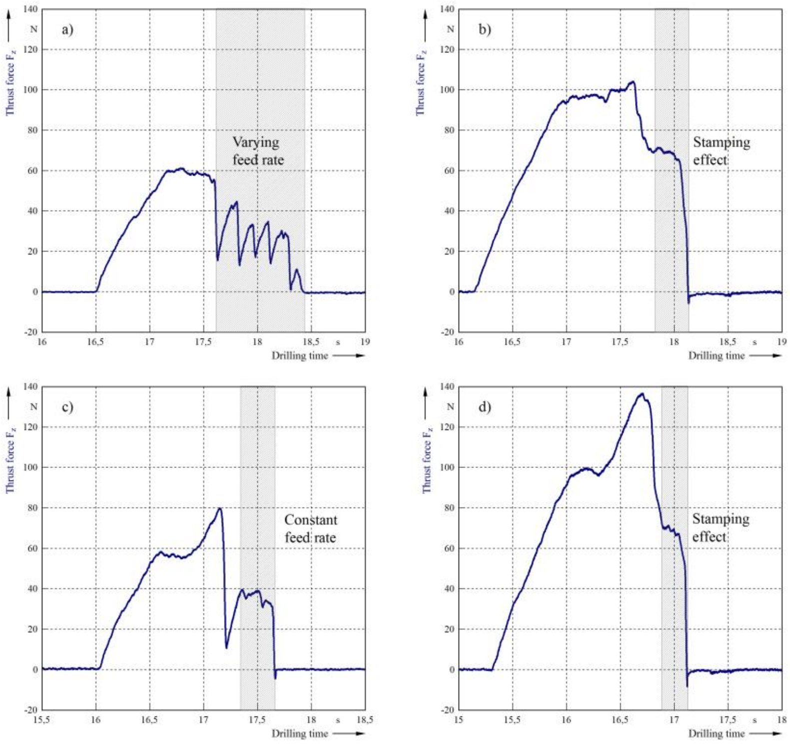

Fig. 6 – Thrust force during unsupported drilling with different point angles and tool wear
a) σ = 70° ; r_β = 20 µm, b) σ = 70° ; r_β = 40 µm, c) σ = 100° ; r_β = 18 µm, d) σ = 100° ; r_β = 35 µm (f = 0.06 mm/rev ; v_c = 100 m/min; t = 4.3 mm ; x = 120 mm ; r_β = cutting edge radius)

In these graphs there are obviously distinctive differences in the secondary drilling stage. The cutting edges for this stage have the same point angle as the cutting edges in the primary drilling stage. Here, a small point angle results in an alternating feed force. As the work piece deflection is proportional to the thrust force, it moves in the same way the force is varying. According to this, the relative feed speed increases when the feed force decreases because the work piece moves into zero position direction at these moments. The small point angle supports this mechanism, as the work piece may slide along the cutting edges in consequence of the high sharpness of the cutting edge and the elastic force of the work piece. Large point angles prevent this mechanism because of the greater similarity to a stamping tool, whereby the tool geometry brings a greater resistance against the work piece movement. This leads to an almost constant relative feed speed in the secondary drilling stage. With higher tool wear this mechanism disappears for all point angles in consequence of the higher cutting forces necessary for the machining process. Hereby, the drilling time for the secondary stage is reduced obviously, because of the comparatively higher raise of the relative feed speed due to the also higher elastic force.

3. ENERGETIC BALANCE EQUATION FOR DRILLING OF UNSTABLE WORK PIECES

To control the drilling process of unstable work pieces a criterion apart from the critical feed force has to be defined. The difficulty in this matter is, that beside the material-specific binding energy, the elastic energy stored in the work piece has an influence on the machining result, too. Concerning the machining process generally, the active work W_e has always to be applied for the destruction of the machined material. This active work consists of two components: The feed work W_f and the cutting work W_c [DIN6584] (see Equ. 1).

$$W_e = W_c + W_f \qquad \textit{(Equ. 1)}$$

During the standard drilling process, the feed work is completely converted into friction and shear energy. In contrast at the drilling of unstable components, a part of the feed work is converted into elastic energy, stored in the work piece. The following correlation can be formulated:

$$W_{f,machine\ tool} = W_{f,work\ piece} + W_{F,work\ piece} \qquad \textit{(Equ. 2)}$$

$W_{f,machine\ tool}$ is the feed work implemented by the machine tool over the whole drilling time, $W_{f,work\ piece}$ is the feed work absorbed by the work piece and transformed into friction or rather shear energy and $W_{F,work\ piece}$ is the elastic energy additionally stored in the work piece. As the cutting force F_c is not directed into the laminates thickness direction, the cutting work W_c is insignificant for the elastic energy. To verify this energy balance, the mentioned feed works and the elastic energy were identified by measuring force and displacement signals during drilling experiments (see Equ. 3 and Equ. 4).

$$W_f = v_f * \int_0^t F_z(\tau) d\tau \qquad \textit{(Equ. 3)}$$

$$W_F = \int_0^f F_z(f) df \qquad \textit{(Equ. 4)}$$

Fig. 7 shows the relevant measurement parameters for the various energy components and visualizes the interactions between drilling tool and work piece. The relative feed speed v_f, the feed force F_z, the deflection f and the torque M_z for drilling an unstable work piece are illustrated in the two diagrams, showing the parameters as a function of the drilling time. The two peaks of the relative feed speed are distinctive. At these moments the work piece moves into the direction of the zero position and as a result, the speed of operation increases. Whenever the work piece is deflected into the feed force direction and the force signal increases slowly, the relative feed rate is at its lowest value. The progression of the deflection shows the proportionality of the work piece movement to the feed force signal. Furthermore the temporary increase of the torque can be obtained clearly when the chisel edge exits the material. At this moment the mentioned reaming process leads to a minimal form deviation of the drilled hole. According to Equ. 2 the energy balance was formed at different moments of the drilling process and as a result, the segmentation of the feed work into different energy parts was verified. Fig. 8 shows the energy balance.

The currently stored elastic energy of the work piece as well as the implemented and the absorbed feed energy are plotted in the diagram. The sum of the two energy parts absorbed by the work piece and the feed work implemented by the machine tool correspond with a deviation of 1.87 %.

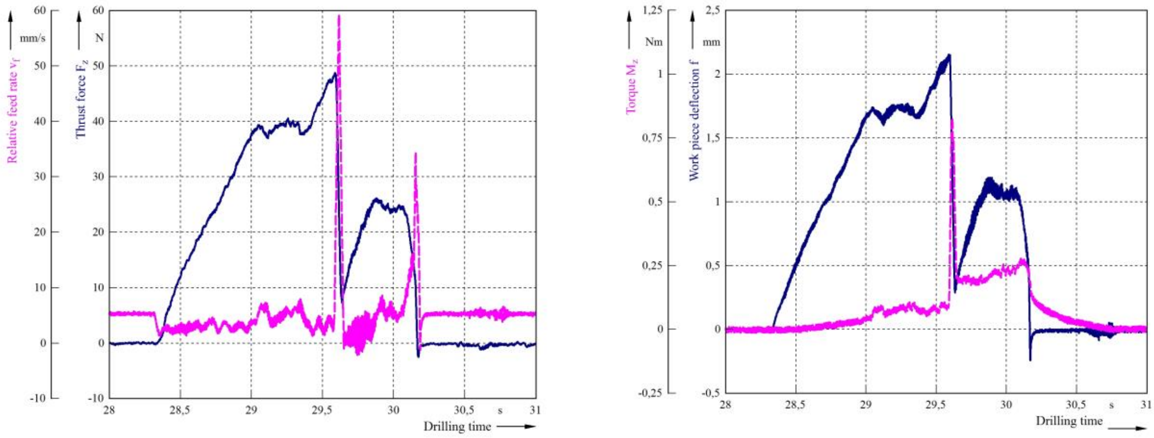

Fig. 7 – Relevant measurement data for the calculation of different energy components at the drilling process (f = 0.06 mm/rev ; v_c = 100 m/min ; σ = 85° ; t = 4.3 mm ; x = 160 mm)

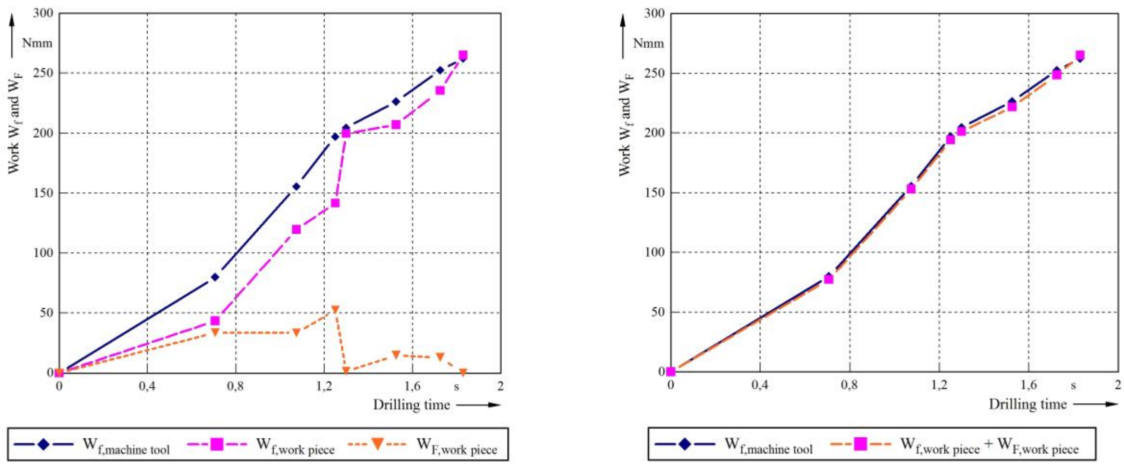

Fig. 8 – Verification of the energy balance
(f = 0.06 mm/rev ; v_c = 100 m/min ; σ = 85° ; t = 4.3 mm ; x = 160 mm)

First investigations to identify a critical value using the elastic energy were carried out by drilling unstable work pieces with worn and unworn drill bits. For this purpose two step drills, one with σ = 70° (B70) and one with σ = 100° (B100), were used. At each of five different states of tool wear, twelve holes were drilled. The unsupported length was varied after three holes respectively and the delamination factor F_d was determined for each hole according to Equ. 5 [Liu12].

$$F_d = \frac{D_{max}}{D_{nom}} \quad \textit{(Equ. 5)}$$

D_{max} is the diameter of the maximum damage and D_{nom} is the nominal diameter of the hole. The test procedure is summarized in Table 2.

Table 2 – Parameters for the experiments with worn drilling tools and unstable work pieces

Tool name	States of tool wear	Unsupported lengths	Machining parameters
B70, B100	25, 75, 150, 225, 300 holes	x = 40, 80, 120, 160 mm	f = 0.06 mm/rev v_c = 100 m/min

Fig. 9 shows the experimental results. For each drill bit the delamination factor F_d is plotted as a function of tool wear or rather the number of drilled holes and the unsupported length x. The dark blue zone marks the test parameters, where holes with a delamination factor of almost 1.0 could be produced. Comparing the two drill bits, with the drilling tool B70 damage-free holes can be drilled in a wider area of test parameters then with the drilling tool B100, which causes a stronger stamping effect.

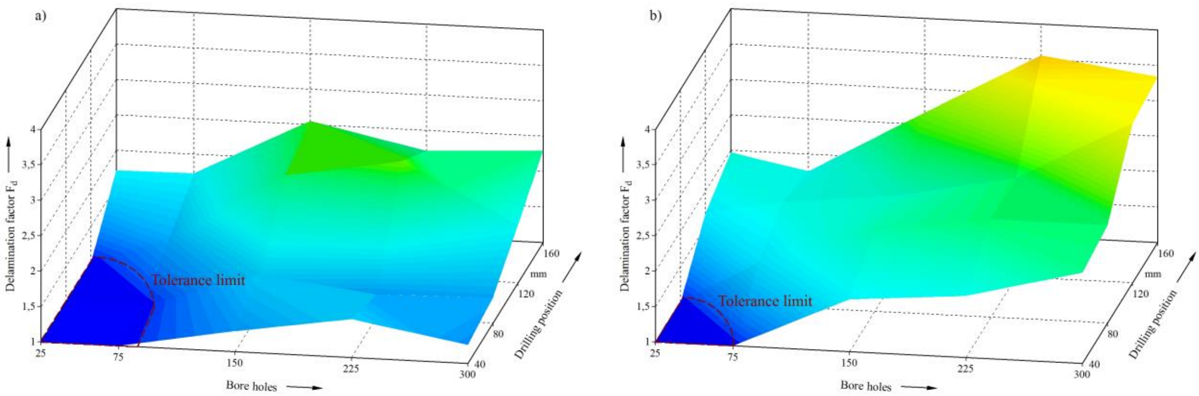

Fig. 9 – Comparison of drilling experiments with different state of wear, unsupported length and point angle a) $\sigma = 70°$, b) $\sigma = 100°$ (f = 0.06 mm/rev ; v_c = 100 m/min ; t = 4.3 mm)

The dependence of the delamination factor from the elastic energy is shown in Fig. 10 for both test series. As the elastic energy stored in the work piece is below 50 Nmm, holes with a delamination factor of 1.5 can be produced independently from the drill bit geometry and the state of tool wear. However, the quality fluctuations of the holes are distinctive. Due to the complex drilling process of unstable work pieces and the materials inhomogeneity, holes with a highly varying delamination factor were produced under the same machining conditions. Because one delaminated fiber should not be evaluated as critical as a multiple ruptured hole, the damage quantification with a simple diameter ratio must be questioned critically. A unified tolerance criterion or damage classification for different damage characteristics does not exist until now. Due to the uncertain effects of delamination on different mechanical stresses, a zero defect tolerance is common in industrial production. Considering the performed test series it would be conceivable to define a critical elastic energy as the limiting criterion for drilling unstable work pieces. But for this purpose an exact specification concerning the tolerable damages and a more flexible quantification system for the damage evaluation have to be developed.

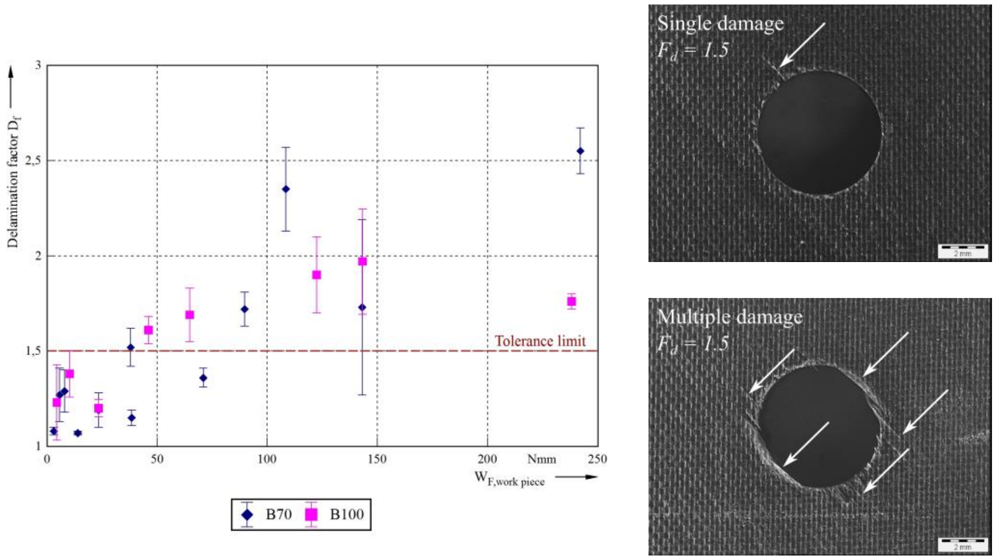

Fig. 10 – Damage evaluation for drilling experiments with worn tools and unstable work pieces depending on the elastic energy (Magnification = 8.4x)

4. Milling of unstable work pieces

First contour milling experiments for trimming unstable work pieces have shown that delamination is not the main damage characteristic here. Fig. 11 presents the comparison of the surface layer damages after machining stable and unstable work pieces, the latter with an unsupported length of 100 mm. As it can be seen from the microscopic pictures, the predominant damages on the work piece cutting edges are frayings. Furthermore the tool geometry has a distinctive influence on the extent of damages. By using a multi-tooth cutter with interrupted cutting edges instead of a tool with two continuous cutting edges, the extent of frayings can be reduced.

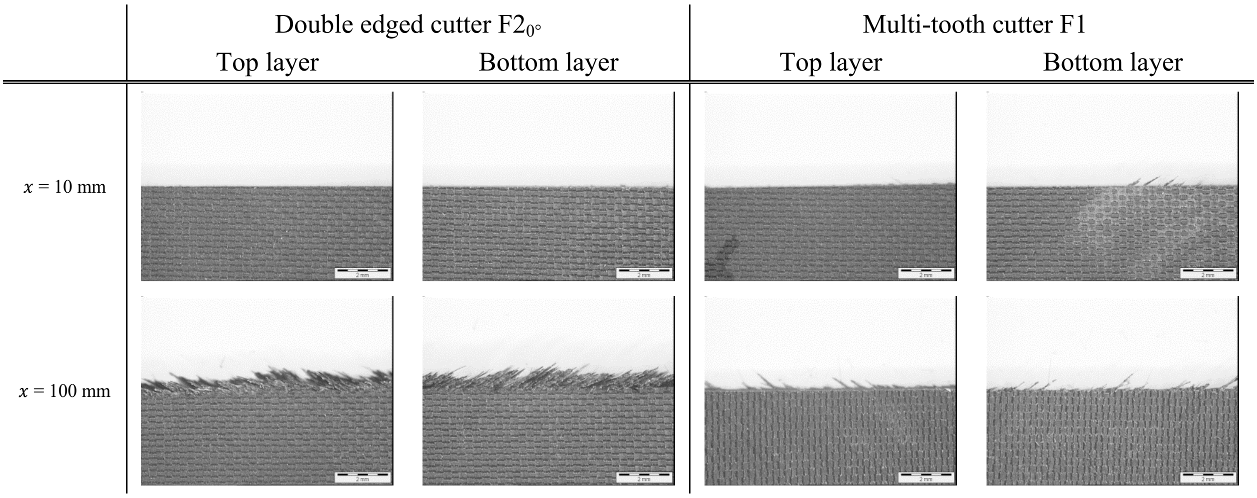

Fig. 11 – Cutting edge quality at trimming unstable work pieces
F1: f = 0.04 mm/rev, v_c = 88 m/min ; F2$_{0°}$: f = 0.07 mm/rev, v_c= 88 m/min
(t = 2 mm ; Magnification = 12.5x ; a_e/d = 1)

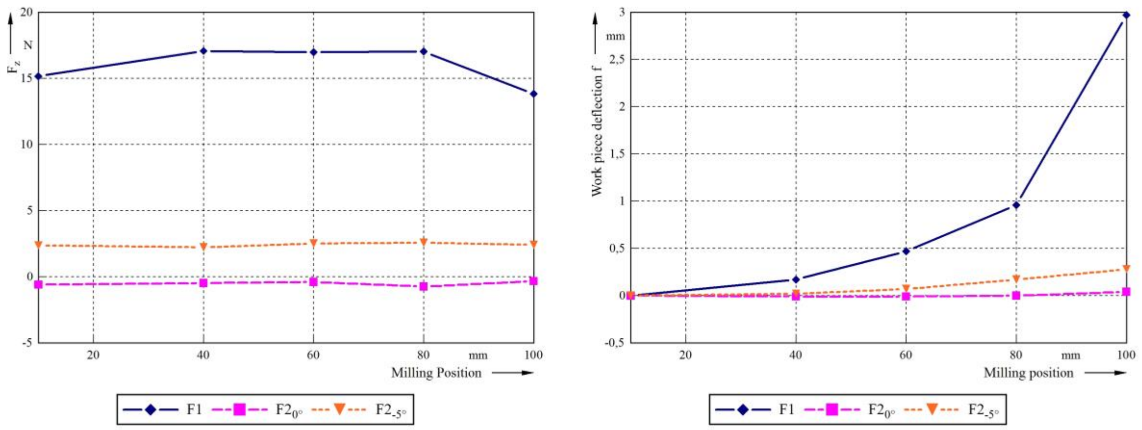

Fig. 12 – Effects of the spiral angle on the force component F_z and the resulting deflection f
F1: f = 0.04 mm/rev, v_c = 88 m/min ; F2$_{0°}$ and F2$_{-5°}$: f = 0.07 mm/rev, v_c= 88 m/min
(t = 2 mm, ; a_e/d = 1)

Considering the machining forces in the laminates thickness direction and the corresponding deformations at different unsupported lengths, it becomes apparent that in contrast to the drilling process the static deflection is not responsible for the emergence of damages. Fig. 12 shows the forces and deflections at different milling positions. The deflection f increases if a work piece is trimmed with a higher spiral angle. Thus a two-edged milling tool with a spiral angle of 0° (F2$_{0°}$) does not cause any force component in the Z-direction whereby the multi-tooth cutter F1 with a spiral angle of 30° provokes the highest force F_z with 15 N. The forces in the Z-direction are almost constant at all milling positions and are far beneath the feed forces of the drilling process. Hence, the interlaminar strength will not be excessed despite additional work piece deflections. Nevertheless, the work piece behaves like a cantilever beam. The compliance increases clearly at a machining position of x = 80 mm and although the force component F_z falls slightly, the deflection triples at x = 100 mm. A FFT analysis of the work piece movement in Z-direction during the whole machining time gives more information about its performance during milling. Fig. 13 compares the dynamic behavior of the work piece, while machining with a two-edged cutter F2$_{0°}$ and the multi-tooth cutter F1.

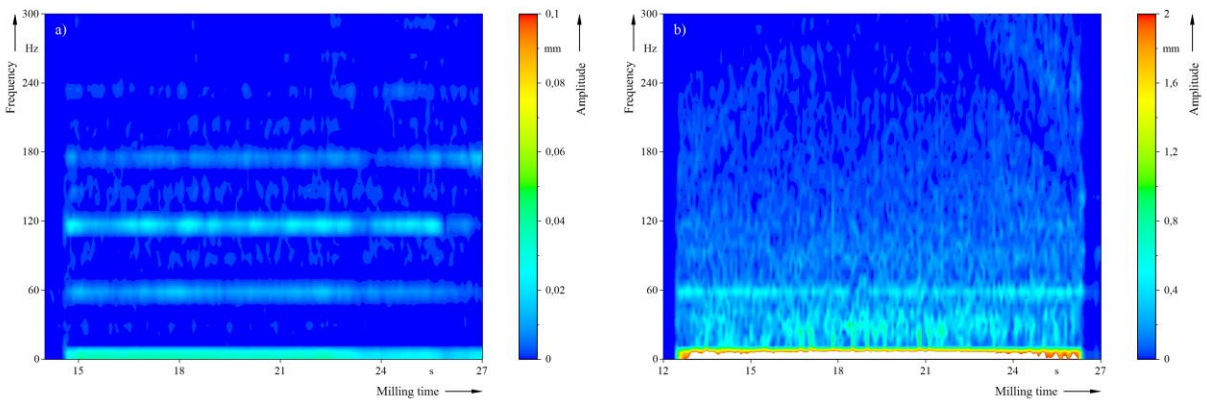

Fig. 13 – FFT of the displacement measurement for trimming unstable work pieces
a) F2$_{0°}$: f = 0.07 mm/rev, v_c= 88 m/min ; t = 2 mm ; x = 100 mm ; a_e/d = 1
b) F1: f = 0.04 mm/rev, v_c = 88 m/min ; t = 2 mm ; x = 100 mm ; a_e/d = 1

Especially for the machining with a two-edged tool $F2_{0°}$, one can obtain the cutter spindle rotational frequency of 58.35 Hz and its multiples. Its double frequency shows the highest amplitude because it corresponds with the tooth engagement frequency of the two-edged cutter. As shown in Fig. 12 and Fig. 13, the static part amounts roughly 0 mm. While milling with a multi-tooth tool F1, the work piece acts in a different way. Predominant excitation frequencies do not appear clearly and the static part is explicitly higher due to the large spiral angle of 30°. The frequency spectrum is broadband and possesses the highest amplitudes. It can be assumed that these oscillations are responsible for the better shearing of frayings.

5. CONCLUSIONS

The investigations concerning the machining of unstable CFRP-structures lead to the following conclusions.

- Generally the machining of unstable work pieces is possible. For the drilling process it has been observed that there is a threshold area beneath which no damages or rather slight damages occur. For the experiments presented in this paper, the work piece compliance has been modified by changing the material thickness and the unsupported length of the bending beam. The next step will be to analyze and extend the investigation series in respect to local work piece compliances. Thereby, the machining quality may be considered independently from the work piece geometry.
- The static and dynamic work piece behavior is strongly influenced by the tool geometry and the current tool wear. Small point angles cause a minor stamping effect although there is an increasing relative feed speed while drilling. Rounded cutting edges lead to higher work piece deflections due to the higher cutting forces. While the static work piece bending plays an important role for the drilling process, for contour milling the work piece vibration is the critical factor. In this connection multi-tooth cutters have a positive effect on the work piece quality.
- The approach to split up the energies taking into account the elastic energy of the work piece has been verified. The threshold area for drilling may be described as a critical elastic energy of the work piece. However, it is required to improve the actual quantifying procedures for damage detection as well as to define universal tolerances and damage classifications, particularly regarding to their impact on the mechanic properties of CFRP.

ACKNOWLEDGEMENTS

The presented studies were performed within the framework of the project “SPANTEC-light” as a part of the research association „Zentren für angewandte Forschung an Fachhochschulen“ (ZAFH), founded by the German federal state Baden-Wuerttemberg. The project and its associates, the Universities of Applied Sciences in Aalen, Mannheim and Ulm, focus on the investigation of the quantitative correlations between material and application properties at machining CFRP.

REFERENCES

[Abr07] Abrão A.M.; Faria P.E.; Campos Rubio J.C. et al. (2007): Drilling of fiber reinforced plastics: A review. *Journal of Materials Processing Technology*, 186 (1-3). S. 1-7.

[Cap04] Capello E. (2004): Workpiece damping and its effect on delamination damage in drilling thin composite laminates. *Jornal of Materials Processing Technology*, 148 (2). S. 186-195.

[Col91] Colligan K. und Ramulu M. (1991): Delamination in surface plies of graphite/epoxy caused by the edge trimming process. *Processing and manufacturing of composite materials*, 27. S. 113-125.

[Enß13] Enßle M. (2013): Zusammenspiel von Fertigungsmittel und Zerspanstrategie bei der Bearbeitung von Faserverbund-Bauteilen für die Luftfahrt. In: *3. IfW-Tagung: Bearbeitung von Verbundwerkstoffen - Spanende Bearbeitung von CFK*. Stuttgart: IfW Stuttgart. S. 65-74.

[Far09] Faraz A.; Biermann D. und Weinert K. (2009): Cutting edge rounding: An innovative tool wear criterion in drilling CFRP composite laminates. *International Journal of Machine Tools and Manufacture*, 49 (15). S. 1185-1196.

[Har12] Hartmann D. (2012): *Delamination an Bauteilkanten beim Umrissfräsen kohlenstofffaserverstärkter Kunststoffe*. Hamburg: Technische Universität Hamburg-Harburg.

[Hoc03] Hocheng H. und Tsao C.C. (2003): Comprehensive analysis of delamination in drilling of composite materials with various drill bits. *Journal of Materials Processing Technology*, 140 (1-3). S. 335-339.

[Hoc05] Hocheng H. und Tsao C.C. (2005): The path towards delamination-free drilling of composite materials. *Journal of Materials Processing Technology*, 167 (2-3). S. 251-264.

[Hoc90] Hocheng H. und Dharan C.K.H. (1990): Delamination During Drilling in Composite Laminates. *Journal of Manufacturing Science and Engineering*, 112 (3). S. 236-239.

[Kha10] Khashaba U.A.; El-Sonbaty I.A.; Selmy A.I. et al. (2010): Machinability analysis in drilling woven GFR/epoxy composites: Part II – Effect of drill wear. *Composites Part A: Applied Science and Manufaturing*, 41 (9). S. 1130-1137.

[Lis13] Lissek F.; Kaufeld M. und Bergmann J.-P. (2013): Aufs Abstützen kommt es an - Bearbeitungskriterien für die Zerspanung labiler Strukturen. *Werkstatt & Betrieb*, 12. S. 36-40.

[Liu12] Liu D.; Tang Y. und Cong W.L. (2012): A review of mechanical drilling for composite laminates. *Composite Structures*, 94 (4). S. 1265-1279.

[Per97] Perrsson E.; Eriksson I. und Zackririsson L. (1997): Effects of hole machining defects on strength and fatigue life of composite laminates. *Composites Part A: Applied Science and Manufaturing*, 28 (2). S. 141-151.

[Tsa03] Tsao C.C. und Hocheng H. (2003): The effect of chisel length and associated pilot hole on delamination when drilling composite materials. *International Journam of Machine Tools and Manufacture*, 43 (11). S. 1087-1092.

[Won02] Won M.S. und Dharan C.K.H. (2002): Chisel edge and pilot hole effects in drilling composite. *Journal of Manufacturing Science and Engineering*, 124 (2). S. 242-247.

[DIN2768] DIN ISO 2768-1:1991-06: *Allgemeintoleranzen - Toleranzen für Längen- und Winkelmaße ohne einzelne Toleranzeinragung*. (ISO 2768-1:1989).

[DIN6584] DIN 6584:1982-10: *Begriffe der Zerspantechnik - Kräfte, Energie,Arbeit, Leistungen*. (ISO 3002/1 - 1977).

CONTACTS

M. Eng. Fabian Lissek lissek@hs-ulm.de
Prof. Dr.-Ing. Michael Kaufeld kaufeld@hs-ulm.de
Univ.-Prof. Dr.-Ing. habil. Jean Pierre Bergmann jeanpierre.bergmann@tu-ilmenau.de